Process Safety and Environmental Protection 164 (2022) 781–793

Contents lists available at ScienceDirect

Process Safety and Environmental Protection

journal homepage: www.journals.elsevier.com/process-safety-and-environmental-protection

Comparison of a variety of physico-chemical techniques in the chronological characterization of a compost from municipal wastes

A.C. Silva [a,b], P. Rocha [a], J. Antelo [c], P. Valderrama [d], R. López [c], D. Geraldo [a], M.F. Proença [a], J.P. Pinheiro [e], S. Fiol [b], F. Bento [a,*]

[a] Department of Chemistry, Center of Chemistry, University of Minho, Campus Gualtar, 4710–057 Braga, Portugal
[b] CRETUS. Department of Physical Chemistry. University of Santiago de Compostela, 15782 Santiago de Compostela, Spain
[c] CRETUS. Department of Soil Science and Agricultural Chemistry, University of Santiago de Compostela, 15782 Santiago de Compostela, Spain
[d] Universidade Tecnológica Federal do Paraná, Campus Campo Mourão (UTFPR-CM), Campo Mourão, Paraná, Brazil
[e] Université de Lorraine, CNRS, Laboratoire Interdisciplinaire des Environnements Continentaux (LIEC), UMR 7360, Vandoeuvre-lès-Nancy F-54000, France

ARTICLE INFO

Keywords:
Compost
Humic-like substances
Stabilization
Circular Economy
Common Dimensions Analysis

ABSTRACT

The degree of stability and maturity of the organic matter are fundamental features of the chemical characterization of compost. These characteristics are related to the extensive formation of aromatic structures and of oxygen-containing functional groups. The increase of the amount of these chemical moieties can be assessed by different analytical methodologies, based on thermal, spectrophotometric, and electrochemical techniques. In order to compare the ability of the most used methodologies to differentiate compost at different composting stages, results from the direct characterization of solid samples and their extracts are reported. A total of 108 parameters from the characterization of a compost at four composting stages were treated by a ComDim analysis. The relevance of the analytical techniques for monitoring composting was established by considering the absolute value of the loadings and that results vary in a single way along the process.

1. Introduction

The improvement of the quality of the environment and the protection of human health depends on the efficient and rational utilization of natural resources and efficient waste management policies promoting the principles of a circular economy. To accomplish these goals the European Union set 2023 as the deadline for the selective collection of biowaste with the aim of recycling by composting and digestion (The European Parliament and the Council of the European Union, 2018). Furthermore, the use of environmentally safe materials produced from biowaste should also be increasingly encouraged by EU countries (The European Parliament and the Council of the European Union, 2008). Thus, compost production and its uses are expected to increase, as a means to fulfill the demand of clean technologies for waste management and the production of an environmentally friendly material (Cerda et al., 2018). Composting converts the organic fraction of the biowaste into a stable product that can be used as a source of nutrients for plant growth and/or improvement of the physical properties of the soil (Haug, 1993). Moreover, compost can be considered as a low-cost adsorbent material for metal removal or immobilization from aquatic and soil systems (Søberg et al., 2019).

Composting can be performed by different methodologies, including vermicomposting, aerobic composting, windrow composting, in-vessel composting, aerated static pile composting and composting using arthropods/insects (Bernal et al., 2009). The selection of the composting technology depends on the amount and type of raw materials and on the available resources (Li et al., 2020; Xu et al., 2022). The temporal evolution of compost is mostly related to the conversion of the most unstable organic compounds, such as sugars, soluble carbohydrates, organic acids, amino acids, and proteins to humic-like substances (HS).

The characteristics of the compost produced depends on the control of multiple parameters, starting from a careful choice of the raw materials (Li et al., 2020). A compost must have well-defined characteristics, such as the content of the organic matter (between 30% and 70%) and an adequate degree of stability and maturity (Haug, 1993). In addition to important requirements, such as, the low concentration in heavy metals, pH value (between 6 and 8), the absence of pathogens and inert materials (stones, glass and plastic) are desirable.

The stability of the compost is related to the refractory nature of its organic matter to undergo further degradation, and maturity is related

* Corresponding author.
E-mail address: fbento@quimica.uminho.pt (F. Bento).

https://doi.org/10.1016/j.psep.2022.06.057
Received 12 August 2021; Received in revised form 18 May 2022; Accepted 26 June 2022
Available online 28 June 2022

to the degree of humification it has undergone. These features are frequently assessed by determining the C/N ratio (organic C, total N) (Inbar et al., 1989), pH and even by means of the variation of the cation exchange capacity (CEC) (Harada and Inoko, 1980). The compost stability and maturity can also be monitored following the structural changes of the organic matter by different techniques, such as Fourier transform infrared spectroscopy (FTIR), thermogravimetric analysis (TGA) and differential scanning calorimetry (DSC). The analysis of the results from these techniques can be straightforward, measuring the weight loss and enthalpies at fixed temperature ranges, or by means of aromaticity indexes that are calculated using band intensity ratios (Inbar et al., 1989).

Alternatively to the characterization of the solid compost, several authors conducted the characterization of the aqueous extracts of compost using extraction and characterization methodologies that are similar to those developed for the characterization of HS of peat (Piccolo and Mirabella, 1987) or soil (Piccolo et al., 1992). The extracts preparation may follow either well defined protocols, such as those from the International Humic Substances Society (IHSS) (Swift, 1996) or other (Cegarra et al., 1994) to isolate and purify the HS or simply by leaving the compost in contact with water for a certain period of time (Gigliotti et al., 2002). The HS isolated from compost are quantified and characterized by elemental analysis (EA) or by spectroscopic (FTIR) and thermal (TGA and DSC) techniques (Hsu and Lo, 1999; Inbar et al., 1992; Melis and Castaldi, 2004). The HS solutions are also characterized by the spectroscopic techniques, UV–vis, ^{1}H NMR and ^{13}C NMR and by their acid-base and metal binding properties (Chin et al., 1994; Gigliotti et al., 2003; Plaza et al., 2005). The aqueous extracts containing the dissolved organic matter (DOM) are also characterized using the same methodologies used for the HS extracts and also by electrical conductivity (EC) (Droussi et al., 2009).

Despite the large amount of information available in literature, there is not a general consensus on the most appropriate method for the assessment of the quality parameters stability and maturity. Although some works report data from different analytical methods, the discussion of results is not oriented towards the comparison of methods, as this is not the aim of those studies. In face of the large number of methods and parameters for compost characterization, we believe that the comparison between all the data from different methods is highly desirable and could start an extended discussion on the suitability of the different methods for the assessment of compost quality parameters.

In the present work we characterize a compost produced from organic urban wastes, at four stages of composting, namely the feedstock material, after one composting cycle, two composting cycles and the final matured compost. This compost was selected due to the increasing production of urban wastes and to the current urgency to decrease their disposed of in landfills, reducing the environmental impacts of the landfills in the quality of the soil, water and air (Kaza et al., 2018). In view of the increasing use of composting as a sustainable solution for urban wastes management, it is relevant to optimize the monitoring of this process. The samples were characterized using data from the solid material and three different extracts. The compost samples were characterized by EA, CEC, FTIR, TGA and DSC, on the other hand, the HS were characterized by EA, UV–vis, ^{1}H NMR, FTIR, TGA, DSC and acid-base and metal binding titrations, whereas the DOM was characterized by EA, EC, UV–vis and acid-base and metal binding titrations. The data set obtained for each sample (including compost, HS and DOM), from different techniques, was analysed by the ComDim (Common Dimension) multi-block tool to highlight the ability of each technique to assess the compost evolution.

2. Material and methods

2.1. Identification of the samples

The compost used in this study was produced from organic urban waste. The raw material combines food wastes (40%) with green wastes (60%) that are obtained from the selective collection. Food wastes are from households, restaurants, canteens, markets and other events such as fairs, festivities, pilgrimages, whereas green wastes are from cemeteries (flowers) and households (grass and pruning). The composting was carried out at industrial level in a tunnel composting system and the composting variables of temperature, oxygen content, humidity and pH were controlled.

Composting was performed in two cycles. In the 1st composting cycle, the feedstock is heated up to 60 °C during 48 h. Then the temperature is set at 50 °C for a period of 15 days. After the 1st cycle of composting, the mixture is sieved with a 60 mm sieve. After this step, the mixture is replaced in the tunnel for a 2nd cycle, identical to the 1st one. After the 2nd composting cycle, the maturation phase occurs and takes between 4 and 6 weeks. The compost samples characterized in this work were collected at four stages of the composting process namely at the entrance of the composting tunnel (t = 0) (UW_0), at the end of the 1st cycle of composting, after 15 days (CUW_{15}), at the end of 2nd composting cycle, after 30 days (CUW_{30}) and after the maturation phase (CUW).

2.2. Preparation of the extracts from compost samples

Three different extracts were prepared from each sample, UW_0, CUW_{15}, CUW_{30} and CUW. The extractions and purification of the HS, namely fulvic-like acids (FA) and humic-like acids (HA) were carried out following the method recommended by IHSS (Swift, 1996). Briefly, samples were extracted with 0.1 mol L^{-1} NaOH under an atmosphere of N_2 at an extractant to compost ratio of 10:1 (v:w). The extracted HS were then separated into HA and FA fractions by acidifying the extract to pH 1 using the 6 mol L^{-1} HCl. The precipitate (HA) and the supernatant (FA) were separated by centrifuging at 2000 rpm for 20 min. The HA fraction was suspended in a solution of 0.1 mol L^{-1} HCl/0.3 mol L^{-1} HF to remove mineral impurities and then dialysed until the elimination of Cl^-. The FA was purified by using an adsorption resin XAD-8, and the alkaline eluate was passed through an H^+-saturated cation exchange resin.

The dissolved organic matter (DOM) and water-soluble inorganic components were extracted using a less aggressive procedure. Succinctly, 2.50 g of the compost were placed in 50 mL of ultra-pure water at natural pH for 5 days in an open system. After 5 days (equilibration time), the supernatants were centrifuged (6000 rpm for 20 min) and isolated for characterization.

2.3. Elemental characterization

The main physico-chemical features of the compost samples, FA, HA and DOM were characterized following the common methodologies for this type of materials. Concisely, C, H, N and S contents were determined by an element analyzer (TruSpec CHN-1000, LecoSC-144DR). Ash content was determined gravimetrically by combustion at 650 °C; oxygen content was determined as O = 100 – (C + N + H + S + ash); oxidizable C was determined by Sauerlandt's method (Walkley, 1947) and C in solution was determined using a total organic carbon analyzer (TOC-L CSN Shimadzu). The concentrations of the major elements were determined by ICP-OES (Perkin-Elmer Optima 3300DV) (in the case of the solid samples, after acid digestion with *aqua regia*); The concentration of P was determined in the compost samples and in the DOM solution by the molybdenum blue method (in the case of the solid samples, after acid digestion with *aqua regia*) (Murphy and Riley, 1962) and the concentration of ammonium in the DOM was determined with a selective electrode (Elit electrode, Nico2000). The Cl^-, F^-, SO_4^{2-}, NO_2^-, NO_3^- ion concentration in DOM was obtained by ion chromatography by Dionex 4500i.

The cation exchange capacity (CEC) was evaluated using an extraction solution of ammonium chloride (Sumner and Miller, 1996). The pH was measured with a combined glass electrode (Crison, pH 0–14). The

electrical conductivity (EC) of the equilibrium solutions were measured using a conductivity meter Crison GLP 32, equipped with a conductivity cell (52–92 model).

2.4. Characterization by TGA and DSC

Compost samples and the FA and HA extracts were characterized by thermogravimetric analysis (TGA) and differential scanning calorimetry (DSC), using a Thermal Analysis Instruments TGA500 and a Perkin Elmer Simultaneous Thermal Analyzer STA 6000, in the temperature range from 30 °C to 800 °C with a heating rate of 10 °C min^{-1}. The analyses were performed on a dry basis using ceramic and aluminium crucibles (60 μL) in air and in N_2 atmospheres, respectively. Samples (30–50 mg) of each compost were obtained from a portion of a sample (1 – 5 g) that was homogenized by manually grinding in an agate mortar.

The quantification of the weight loss was carried out by the TGA curves after careful identification of the temperature ranges corresponding to each process using the derivative thermogravimetric (DTG) curve. The baseline correction was performed using an empty pan. The enthalpies were calculated by integrating the area below the DSC curve in each temperature range, between 30 °C and 800 °C, drawing a horizontal baseline (heat flow 0) from 30 °C to 800 °C, with the aid of Origin 2019b software.

The uncertainties associated with results from TGA and DSC were estimated from replicates of independent measurements. The values of the relative standard uncertainty associated with the values of weight loss (WL_1, WL_2, WL_3, WL_4), total weight loss (TWL) and residue (Res) were estimated from the analysis of triplicates of 10 samples, for a total of 20 degrees of freedom (N = 30–10). The estimated values of relative standard uncertainties were 26% for WL_1, 7.8%, for WL_2, 8.8% for WL_3, 30% for WL_4, 3.0% for TWL and 6.5% for *Res*. For the calorimetric measurements, the relative standard uncertainty of the heat values at each temperature range (H_1, H_2, H_3) were estimated from the analysis of duplicates of 10 samples for a total number of degrees of freedom of 10 (N = 20–10). The estimated values of relative standard uncertainties were 23% for H_1, 13%, for H_2 and 4.7% for H_3.

2.5. Characterization by ATR - FTIR spectroscopy

Compost samples and the FA and HA extracts were characterized by ATR-FTIR spectroscopy. The FTIR spectra were recorded in the transmission mode using a Jasco FT/IR - 4100 Spectrometers with an ATR Specac Golden Gate, in a wavenumber range of 600–3800 cm^{-1} and corrected against ambient air as background. Each spectrum is the results of 64 scans with a resolution of 1 cm^{-1}. Samples of each compost were obtained from a portion of a sample (1 – 5 g) that was homogenized by manually grinding in an agate mortar. The spectra were corrected with the baseline and submitted to a deconvolution process using Origin 2019b software. In the deconvolution process, the compensation of the intrinsic linewidths is made in order to solve overlapping bands.

2.6. Characterization by UV–vis

The UV–vis spectroscopy was used to characterize the FA, HA and DOM extracts of all compost samples at different concentrations. A Jasco V-530 spectrophotometer was used to measure the absorbance of the solutions at a fixed wavelength (280 nm). This wavelength was selected as the coefficient of molar absorptivity at 280 nm (ε_{280}) is correlated by semi-empirical relationships with aromaticity (% aromaticity = 0.05 x ε_{280} + 6.74) and with the molar mass (molar mass = 3.99 x ε_{280} + 490) (Fuentes et al., 2006).

2.7. Characterization by ^{1}H NMR spectroscopy

The ^{1}H NMR spectroscopy was used to characterize the FA and HA extracts of all compost samples. ^{1}H NMR was carried out using a 400 MHz Bruker Avance II spectrometer NMR. Chemical shifts (δ) are given in parts per million (ppm), downfield from tetramethylsilane (TMS), and coupling constants (J) in hertz (Hz). The HS solutions were obtained by dissolving 5 mg of the sample in 800 μL of deuterated water (Merck) and the pH was adjusted to 12 with 40% NaOD (Sigma-Aldrich).

2.8. Characterization by acid-base titrations

Acid-base titrations were conducted for DOM solutions and both the HA and FA extracts (0.1 g HS/L), following the protocol proposed by López et al. (López et al., 2003). Fully automated acid-base titrations were performed using a Crison microBU 2031 burette and a Crison 2002 pH-meter connected to a computer using a home-made software. The titration of the DOM was conducted at 0.1 mol L^{-1} ionic strength in KNO_3 (Merck) while titrations of the HA and FA extracts were conducted at 0.1 mol L^{-1} to compute both the electrostatic and chemical protonation parameters: protonation constants of the carboxylic and phenolic groups, K_i, the abundance of each type of group, M_i, and the width of the distribution of the K_i values, m_i. Because of the relatively high pH values of the equilibrium solutions, two aliquots were taken from each sample to characterize the protonation (titration with 0.1 mol L^{-1} HCl (Panreac)) and deprotonation processes (titration with 0.1 mol L^{-1} KOH (Merck)).

2.9. Determination of Cd complexation by AGNES

Voltammetric measurements were carried out with an Autolab PGSTAT30 potentiostat attached to a Metrohm 663 VA Stands and to a computer by means of the GPES 4.9 software (EcoChemie). The electrochemical cell (25 mL) was composed by a thin film mercury electrode deposited at a glassy carbon rotating disk electrode (Metrohm, 6.1204.300) as the working electrode, a carbon rod (Metrohm, 6.1248.040) auxiliary electrode and an Ag/AgCl reference electrode (World Precision Instruments, Driref-5). The pH measurements were performed using a glass combined electrode (HI11311, Hanna instruments) connected to a pH meter (Thermo Scientific, Model CyberScan pH 510). The preparation of the mercury thin film followed the protocol proposed by (Rocha et al., 2010).

AGNES is an electroanalytical technique that quantifies the free metal ions present in solution quite similarly to an ion selective electrode (Galceran et al., 2004). This technique was used to determine the free cadmium ions in presence of the different FA, HA and DOM extracts These determinations were carried out in duplicate in presence of a fixed amount of the corresponding extract and successive additions of known aliquots of a standard cadmium solution (1000 mg L^{-1}).

All solutions were prepared using ultrapure water (Milli-Q System, Millipore). Cadmium solutions were prepared from a 1000 mg L^{-1} cadmium standard solution in 0.5 mol L^{-1} HNO_3 (Merck). The electrolyte solutions were prepared by dilution of $NaNO_3$ (Merck) and HNO_3 (PanReac Applichem). In the complexation experiments, the ionic strength of the solutions was adjusted to 12 mmol L^{-1} using 1.0 mol L^{-1} HNO_3 (PanReac Applichem) and 1.0 mol L^{-1} $NaNO_3$ (Merck). The pH of the cell solutions was adjusted to pH 7.0 using 0.10 mol L^{-1} NaOH. The solutions (400 mg L^{-1}) of the (i) FA and (ii) HA were prepared by placing 20 mg of the corresponding extract in 50 mL of ultra-pure water at (i) natural pH or (ii) at pH 9.0 and with an argon purge (in order to avoid carbonation reactions) and stirring for about 12 h. The equilibrium solutions were diluted before the electrochemical assay, according to the respective values of dissolved organic carbon (DOC).

2.10. Statistical analysis (multi-block data analysis)

Common Dimensions (ComDim) belongs to the family of multiblock components analyses, being attractive due to the possibility of integrating and evaluating multiple information describing the same samples, highlighting, in an exploratory way, interesting features of multiple data blocks (Cariou et al., 2019). The ComDim-based method calculates

a weighted sum of the sample variance-covariance matrix of each block, followed by the extraction of the first principal component standardized and named Common Component (CC). Then, the global and local components are extracted from multiple blocks of data sequentially and iteratively calculate the weight or salience of each block for the calculated CC. After calculating the first CC, each original data block matrix is deflated, and the procedure is repeated for calculating the second CC, and so on. In summary, the salience indicates the importance of each block in the construction of the CC, each CC is the first PC of a weighted sum of the sample variance-covariance of deflated matrices, and the importance of each block and its inter-block relationships is graphically shown through saliences plot (Cariou et al., 2019; Rocha Baqueta et al., 2021; Bouveresse et al., 2011; Qannari et al., 2000). In other words, this unsupervised multiblock analysis determines a common space for all different data blocks, in which each data block has a specific contribution ("salience") to the determination of each dimension of this common space. For this purpose, it is extracting, in a sequential way, global and local (block) components that recover the maximum of the total variance in the set of data blocks (Cariou et al., 2019). Besides improving the results interpretability, with the salience result it is possible to verify the relationship between different analysis types and/or blocks (Rocha Baqueta et al., 2021). Another important result from the ComDim analysis are the informative graphs showing similarities and differences between the samples through scores, and which variables are responsible for the similarities and differences observed in the samples through loadings. In this way, clustering of samples reveals similarities between the samples, while no clustering shows differences. On the other hand, the clustering of variables indicates inter-variable relationships (Rocha Baqueta et al., 2021; El Ghaziri et al., 2016; Rosa et al., 2017).

ComDim analysis was implemented through the Matlab software R2007b and is mathematically step by step described in detail elsewhere (Bouveresse et al., 2011; El Ghaziri et al., 2016).

3. Results and Discussion

Results and discussion from the characterization of the compost samples (UW_0, CUW_{15}, CUW_{30} and CUW) obtained at different composting stages are presented in two sections. Results obtained from the direct analysis of the compost samples are presented in the 1st section, whereas results from the characterization of the HA and FA and of the DOM (equilibrium solutions) are shown in the 2nd section.

3.1. Compost characterization

3.1.1. Elemental analysis and cation exchange capacity

Elemental characterization of compost, particularly carbon, nitrogen and the carbon to nitrogen ratio (*C/N*) is important for both the feedstock and compost (Huang et al., 2004). The monitoring of these parameters at the initial stage of composting is important to control the optimal conditions for microbial growth (Guo et al., 2019) and increase the efficiency of composting. As compost is used as a source of nutrients for soil, other parameters, such as sulfur and organic carbon (C_{oxi}, oxidizable carbon) are also commonly characterized (Awasthi et al., 2020). These parameters from the raw material and compost at three composting stages are presented in Table 1. Data from these samples show a steady decrease for both *C* and *C/N* values, which is in accordance with the reported results and is related to the CO_2 release during composting. Although a C/N value between 20 and 30 is traditionally suggested to ensure that the humification rate proceeds at a high rate (Diaz et al., 2020), the raw material (sample UW_0) has a *C/N* value of 18.6 that is considered low. This value this value is however higher than 15 which was shown to be acceptable for urban waste mixtures (Huang et al., 2004).

The cation exchange capacity (*CEC*) is an important parameter for the characterization of organic matter as it is related to the amount of negative charges present at the surface of the solid matrix, that is evaluated from the extent to which cations are exchanged. Although the *CEC* is one of the parameters employed to describe the properties of soils it has also been widely used to monitor the evolution of compost (Saharinen, 1998). By comparison of results from CUW_{15} and CUW_{30} with the final matured compost (CUW) (Table 1), an increase of the *CEC* is observed, similarly to the previously described (Harada and Inoko, 1980). This increase is assigned to the formation of carboxylic and phenolic functional groups that occurs by the humification process (Azim et al., 2018). Although this trend is observed in our results for the last 3 samples (CUW_{15}, CUW_{30} and CUW), the uncomposted material (UW_0) exhibited an abnormal high value of *CEC*. The origin of this result may be associated with an initial decrease of the complexing functional groups, due to the occurrence of mineralization reactions that take place at the initial stages of the composting process (Wu et al., 2017).

Table 1
Data of elemental composition (from EA) and related to molecular structure (from CEC, UV–vis, ATR-FTIR, TGA and DSC) of the raw material (UW_0) and of the solid compost at three composting stages (CUW_{15}, CUW_{30} and CUW) (blocks 1, 2).

Block	Technique	Parameter	UW_0	CUW_{15}	CUW_{30}	CUW
		C (%)	40.4	38.9	35.2	34.0
		C_{oxi} (%)	38.6	36.9	34.8	29.3
		N (%)	2.54	2.81	2.73	2.71
1	EA	S (%)	0.204	0.264	0.286	0.222
		C/N	18.6	16.1	15.0	14.7
		C_{oxi}/C	95.4	95.0	98.9	86.1
2	ATR-FTIR	$I_{1630/12925}$	0.91	1.44	3.69	3.40
		$I_{1630/12845}$	1.30	2.03	6.32	19.8
		$I_{1540/2925}$	0.71	1.16	1.67	2.34
	TGA	WL_1@air (%)	7.8	8.8	9.3	9.4
		WL_2@air (%)	43	40	32	28
		WL_3@air (%)	28	29	29	27
		WL_4@air (%)	2.1	2.2	3.4	7.4
		Res @air (%)	18	20	25	28
		WL_3@air/ WL_2@air	0.64	0.72	0.91	0.96
		$WL_1@N_2$ (%)	6.8	1.7	2.4	4.9
		$WL_2@N_2$ (%)	38	50	36	20
		$WL_3@N_2$ (%)	13	7	7	27
		$WL_4@N_2$ (%)	5.9	5.8	4.6	10
		Res $@N_2$ (%)	36	37	50	38
		$WL_3@N_2$/ $WL_2@N_2$	0.35	0.13	0.20	1.34
		$WL_3@N_2$/ WL_3@air	0.47	0.23	0.24	0.99
	DSC	H_1 (kJ g^{-1})	1.72	1.89	1.88	1.57
		H_2 (kJ g^{-1})	-2.70	-2.49	-2.01	-2.08
		H_3 (kJ g^{-1})	-4.50	-4.39	-4.66	-4.65
		H_3/H_2	1.7	1.8	2.3	2.2
	Cation exchange capacity	*CEC* (cmol (+) kg^{-1})	128	96.3	109	167

3.1.2. Differential scanning calorimetry and thermogravimetric analysis

The thermal characterization of the samples at the different composting stages was performed by DSC and TGA. These two techniques are commonly used in the characterization of natural materials containing humified matter as they provide important information on the stabilization degree of the organic matter.

The DSC curves (supplementary material) exhibit a minor endothermic process, at the lower temperature limit (close to 100 °C), usually

ascribed to dehydration reactions. Two major regions, corresponding to the overlap of exothermic processes related to the decomposition of recalcitrant and extra-recalcitrant substances, respectively, are also visible (supplementary material). These two exothermic peaks, close to 320 °C and to 500 °C, are characteristic of stabilized organic matter (Fernández et al., 2012). The DSC curves for the different materials exhibit marked differences in shape and height, nevertheless the values obtained by integration of curves in the three temperature ranges (H_1, H_2, H_3) reveal minor variations (Table 1). This outcome may be due to the complexity of the materials and of the large number of reactions that take place at close temperatures, making it rather difficult to isolate and quantify the contribution of the separated processes. The value of H_3, the enthalpy of the overlapped processes that take place at the higher temperature range (associated with the decomposition of the extra-recalcitrant structures) is higher than the H_2, corresponding to the processes that take place at temperatures close to 320 °C, associated to the decomposition of the recalcitrant structures, for all the samples. The ratio between these two enthalpy values H_3/H_2 gradually increases (Table 1) and therefore we propose the use of this ratio as an additional parameter for monitoring the composting progress.

The TGA curves and the corresponding DTG curves from the samples at different stages of composting recorded under an atmosphere of air are shown in Fig. 1A. Although the air atmosphere is more frequently used for the characterization of compost and soil, we performed the thermal characterization under air and N_2 atmospheres in order to get information on the relative importance of the oxidative reactions in the decomposition process. The TGA curves recorded under the air atmosphere contain three main weight loss processes, WL_2 (177–400 °C), WL_3 (400–620 °C) and WL_4 (620–800 °C) and a secondary one at the limit of the lower temperatures, WL_1 (30–177 °C). Where the decomposition processes related to WL_2 and WL_3 can be associated to the enthalpy values H_2 and H_3 from the recalcitrant and extra-recalcitrant matter. Regarding the total weight loss, there is a gradual decrease of this quantity throughout composting, which results in an increase in the final residue recovered from the TGA experiments performed in both atmospheres. This trend is expected due to the stabilization of the organic matter that takes place during the composting process (Melis and Castaldi, 2004). A more detailed analysis of the TGA results can be performed by means of the corresponding DTG curves (Fig. 1A) that exhibit wide and not symmetrical peaks for each of the four processes, particularly the 3rd peak that is rather bumpy. This outcome indicates that these processes result from the overlap of more than one single process. The values of weight loss from the four regions above identified are displayed in Table 1. The values of WL_1 (associated to dehydration and desorption processes) and WL_3 (related to the degradation of complex aromatic structures, such as lignin, complex aromatic structures, and humic substances) (Som et al., 2009) do not show a notable variation considering the uncertainty associated with these results. The steadiness of WL_3 may result from the fact that the decrease of the extent of the degradation of the uncomposted matter (such as aromatic structures and lignins) is compensated by an increase of the extent of the thermal decomposition of the composted matter (such as humic-like complex structures). The values of WL_2 and WL_4 show a steady variation. The decrease of WL_2 is related with the progressive decrease of the easily biodegradable aromatic structures (carbohydrates moieties and aliphatic compounds) (Som et al., 2009), while the increase of WL_4 is due to the formation of inorganic species, such as carbonates (Melis and Castaldi, 2004; Som et al., 2009). The ratio WL_3/WL_2, that can be taken as a measure of the relative amount of the thermally more stable fraction of organic matter compared to the least stable (Dell'Abate et al., 2000), was calculated and is depicted in Table 1. This ratio shows a continuous increase during composting that is mainly associated with the decrease of WL_2.

The comparison of results obtained under both atmospheres (N_2 and air) is highlighted in Fig. 1D. As most of the data points of the weight loss values (open symbols) are found below the 1:1 line, indicating that the decomposition extent tends to be larger in the presence of oxygen, the values of the residue (full symbols) of all samples are larger for the N_2 atmosphere. Besides, the value of the residue of CUW in air displays the lower distance to the 1:1 line. The presence of higher amounts of oxygen

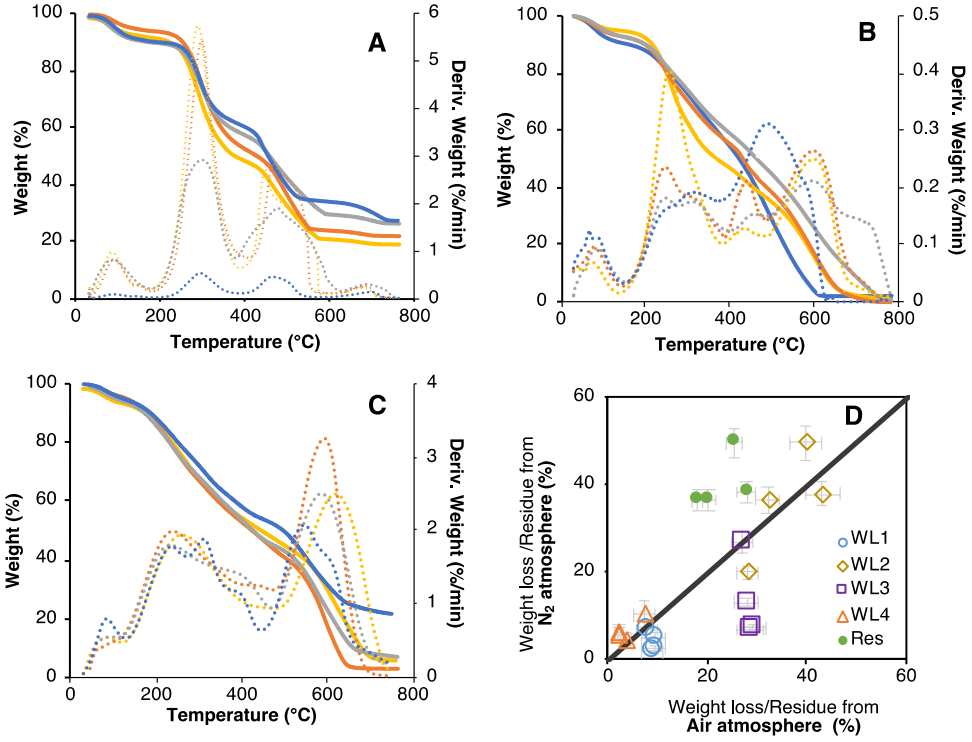

Fig. 1. TGA and DTG curves obtained in air atmosphere for: solid compost (A), HA (B) and FA (C). Comparison of TGA data obtained under the atmospheres of N_2 and air (D). Results of samples from different stages of composting: (●) UW_0, (●) CUW_{15}, (●) CUW_{30}, (●) CUW.

structures in this sample may justify that the extent of its thermal decomposition by pyrolysis is like that from combustion. As the values of WL_1 are larger under the air atmosphere, this process should result from the overlay of processes such as the endothermic processes of dehydration and desorption (as previously discussed) via oxidative pathways. With respect to WL_3, that corresponds to the thermal decomposition of the most stabilized organic matter, significantly higher values were obtained for all samples in the presence of oxygen, except for CUW, whose point is located over this line. This result indicates that the thermal decomposition of CUW, that has undergone extensive oxidation reactions, may take place by pyrolysis. The value of WL_3, that results from the decomposition of uncomposted and composted matter, depends significantly on the nature of the TGA atmosphere. While WL_3 in N_2 varies significantly, in air it is almost constant. Under the N_2 atmosphere, WL_3 should mainly be due to the decomposition of the composted matter by pyrolysis, that increases throughout composting, in opposition to air, where the weight loss may include the contribution of the combustion of uncomposted and composted matter.

The values of WL_2 and WL_4 obtained under the two atmospheres are rather similar, indicating that the thermal decomposition of the easily biodegradable aromatic structures and of inorganic carbonates occurs to a similar extent.

Following this reasoning, we proposed a ratio between the values of WL_3 obtained in the two atmospheres (Table 1). The ratio for CUW is the highest, close to 1, while samples CUW_{15}, CUW_{30} display values that are much lower, both close to 0.2. Although the expected ratio for the starting material (UW_0) was lower than 0.2, a value of 0.5 was obtained. This result can be due to the difficulty of measuring WL_3 from the TGA obtained under N_2 atmosphere due to the overlap of the processes 2 and 3, particularly for UW_0.

3.1.3. ATR-FTIR spectroscopy

The ATR-FTIR spectra of the samples obtained at different stages of composting are shown in Fig. 2A. The spectra of the samples obtained at different stages of composting shows important features that are present in all samples, namely: a band at 3320 cm^{-1} that can be ascribed to C-H bonds and to O-H of alcohols, phenols or O-H carboxyl and also to N-H vibrations in amide functions (Ouatmane et al., 2000); two characteristic bands at 2925 and 2845 cm^{-1} that may be attributed to asymmetric and symmetric vibrations of C-H stretching of CH_3 and CH_2 groups (Kaiser and Ellerbrock, 2005); a band centred at around 1640–1630 cm^{-1} that may be attributed to aromatic C═C and C═O stretching of amide groups and quinonic C═O and/or C═O of H-bonded conjugated ketones (Ouatmane et al., 2000); a band at 1540 cm^{-1} that may be ascribed to secondary amides (Ouatmane et al., 2000); two bands between 1440 and 1420 cm^{-1} that can be associated to the O-H deformation and C-O stretching of carboxylic group, C-H deformations of CH_3 and CH_2 groups and/or asymmetric stretching of COO^- groups (Fuentes et al., 2007); and a band at around 1020 cm^{-1} that may be due to the combination of C-O stretching of polysaccharides, in addition to Si-O-Si bonds of silica and to the group Si-O-C (Ouatmane et al., 2000).

Using the absorption intensity values of the most significant bands of the ATR-FTIR spectra (2915, 2845, 1630 and 1540 cm^{-1}) associated to aliphatic and aromatic moieties, three ratios were calculated to define the aromaticity indexes (Inbar et al., 1989): $I_{1630/2925}$, $I_{1630/2845}$ and $I_{1540/2925}$. The values of these ratios increase throughout the composting process (Table 1), associated to a net increase of the aromaticity degree of the chemical structures related to the formation of HS, such as HA and FA, and the decomposition/transformation of aliphatic components such as polysaccharides and alcohols. These ratios are regarded as indicators of maturity and stability of the organic matter in transformation (Hsu and Lo, 1999).

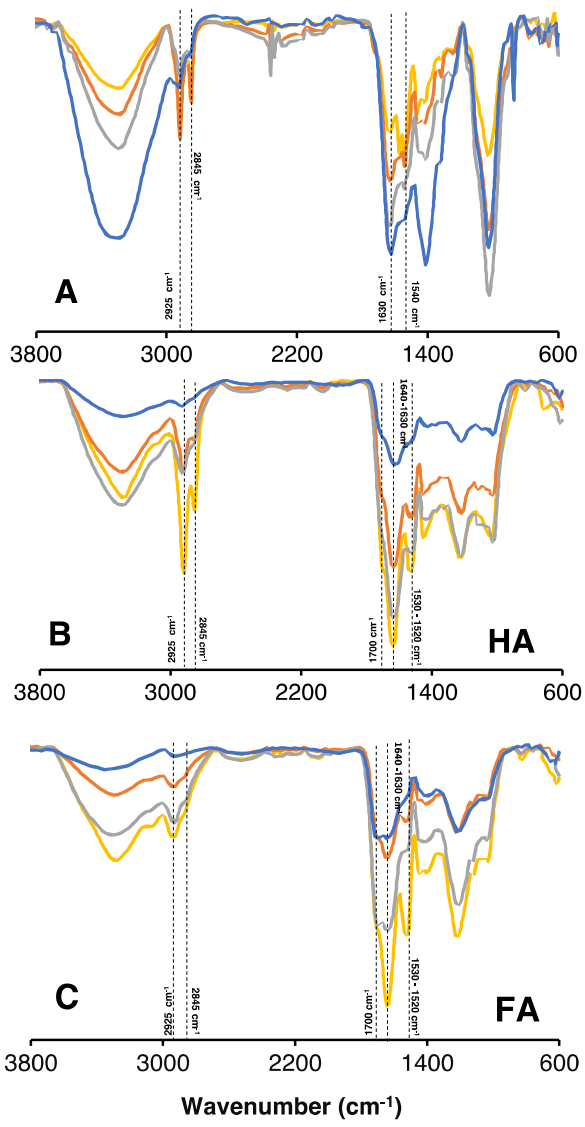

Fig. 2. ATR-FTIR spectra of: solid compost (A), HA (B) and FA (C). Spectra of samples from different stages of composting: (●) UW_0, (●) CUW_{15}, (●) CUW_{30}, (●) CUW.

3.2. Characterization of the extracts of HS and DOM

3.2.1. DOM physico-chemical characterization

Values of the dissolved organic carbon (*DOC*), electrical conductivity (*EC*) and *pH*, are reported in Table 2. The values of *DOC* show a marked decrease when the feedstock material (UW_0) is compared with the matured compost (CUW). This effect is identical to the previously reported by (Wang et al., 2014) and is attributed to the degradation of easily biodegradable organic matter, especially carbohydrates, organic acids and hemicellulose. The *EC* of the DOM extract also tends to decrease, with the most pronounced variation occurring during the first cycle of composting. The *pH* values show an increasing trend throughout the composting process, of about 0.4 units after the first cycle of the composting process, followed by an increase of approximately one unit, in the second cycle. The maturation process does not seem to significantly affect this parameter.

3.2.2. HS physico-chemical characterization

Considering that the organic matter humification occurs throughout composting, the amount of FA and HA extracted should increase from UW_0 to CUW. Furthermore, a negligible amount of these substances

Table 2
Data of elemental composition (from EA, wet chemistry analysis, ion chromatography, pH and EC) and related to molecular structure (from UV–vis, ATR-FTIR, ^{1}H NMR, TGA, DSC, acid-base and metal binding titrations) of HA, FA and DOM (blocks 3–8).

Block	Technique	Parameter		UW_0	CUW_{15}	CUW_{30}	CUW
5, 7	EA	C (%)	HA	59.8	54.4	54.6	54.5
			FA	52.2	52.3	50.3	40.8
		N (%)	HA	5.45	5.44	5.64	6.74
			FA	6.16	5.17	4.25	4.37
		H (%)	HA	7.97	6.9	5.75	6.14
			FA	6.17	6.1	5.65	6.02
		S (%)	HA	0.69	0.9	0.91	0.91
			FA	0.97	0.77	1.05	0.96
		O (%)	HA	26.1	32.4	33.1	31.7
			FA	34.6	35.7	38.8	47.8
		C/N	HA	13	12	11	9.4
			FA	9.9	11.8	13.8	10.9
		O/C	HA	0.33	0.45	0.45	0.44
			FA	0.5	0.5	0.6	0.9
		H/C	HA	1.6	1.5	1.3	1.4
			FA	1.4	1.4	1.3	1.8
	Wet chemistry analysis	DOC (mg L^{-1})	DOM	1187	429	430	548
		C_{oxi} (%)		6.2	2.3	2.5	3.7
	Ion chromatography	Cl^- (mg L^{-1})		415	352	579	392
		F^- (mg L^{-1})		0.12	0.08	0.08	0.18
		SO_4^{2-} (mg L^{-1})		43.1	30.0	22.8	105
		PO_4^{3-} (mg L^{-1})		110	80.4	60.3	29.5
3		NO_2^- (mg L^{-1})		1.71	2.72	4.18	3.94
		NO_3^- (mg L^{-1})		2.56	1.05	1.28	5.21
		NH_4^+ (mg L^{-1})		10.8	13.2	10.1	7.78
		NH_4^+/NO_3^-		4.22	12.56	7.85	1.49
	Potentiometry	pH		6.41	6.81	7.93	7.69
	Conductivity	EC (μs cm^{-1})		3870	3030	3300	2840
6, 8	Extraction yield	Yield (g kg^{-1})	HA	33.1	19.8	21.9	21.1
			FA	2.2	2.7	2.4	3.3
4, 6, 8	Uv-vis	ε_{280} (L $molC^{-1}$ cm^{-1})	HA	212	293	366	513
			FA	186	233	358	419
			DOM	75.5	166	237	280
6, 8	^{1}H NMR	Ratio	HA	8.7	7.3	6.7	4.8
		Aliphatic/Aromatic protons	FA	6	6.4	6.4	5.6
		Ratio	HA	1.7	7	4.4	5.4
		H_2O/ Aliphatic + Aromatic protons	FA	10	8	11	16
6, 8	ATR-FTIR	$I_{1630/12925}$	HA	1.6	2	2.5	4.7
			FA	2.7	2	2.1	7.6
		$I_{1630/12845}$	HA	2.7	3	3.8	4.3
			FA	3.5	4.8	3.1	9.1
		$I_{1540/2925}$	HA	1	0.75	1.4	2
			FA	1.8	1.3	1.3	1.3
6, 8	TGA	WL_1 @air (%)	HA	4.1	5.5	5.2	10
			FA	2.5	3.7	2.7	6.4
		WL_2 @air (%)	HA	48	28	31	31
			FA	44	47	49	38
		WL_3 @air (%)	HA	46	61	56	57
			FA	48	45	42	36
		Res@air (%)	HA	1.2	5.5	6.4	2
			FA	4.1	2.6	6.1	22
		WL_3 @air/WL_2 @air	HA	1	2.2	1.8	1.8
			FA	1.1	1	0.9	0.9
6, 8	DSC	H_1 (kJ g^{-1})	HA	0.31	0.17	0.3	0.27
			FA	0.66	0.2	0.23	0.47
		H_2 (kJ g^{-1})	HA	-0.56	-0.3	-1.13	-1.25
			FA	-1.51	-0.64	-0.81	-3.08
		H_3 (kJ g^{-1})	HA	-0.64	-0.43	-1.29	-4.52
			FA	-1.49	-2.3	-2.02	-2.52
		H_3/H_2	HA	1.14	1.45	1.13	3.62
			FA	0.99	3.62	2.49	0.82
4, 6, 8	Acid-base properties	M_1 (mmol/g_{HS})	HA	2.2	2.3	2.7	2.9
			FA	2.4	3.4	3.6	3.7
		M_1 (mmol/$g_{compost}$)	DOM	0.42	0.05	0.03	0.06
		M_2 (mmol/g_{HS})	HA	1.1	1.2	1.2	1.8
			FA	2.2	1.6	1.5	1.5
		M_2 (mmol/$g_{compost}$)	DOM	0.16	0.24	0.25	0.18
		M_3 (mmol/$g_{compost}$)	DOM	0.27	0.22	0.21	0.19
		log K_1	HA	6.1	5.3	5.2	4.7
			FA	4.2	4.3	4.1	4
			DOM	4.5	3.99	3.57	3.69
		log K_2	HA	10.2	9.9	9.9	9.7
			FA	8.4	9.1	9.5	9.4

(*continued on next page*)

Table 2 (*continued*)

Block	Technique	Parameter		UW_0	CUW_{15}	CUW_{30}	CUW
			DOM	6.05	6.54	6.65	6.51
		log K_3	DOM	9.73	10.06	10.08	10.11
4, 6, 8	Metal binding properties	ML_{low} (L μg C^{-1})	HA	0.75	1	2.4	5.9
			FA	0.52	0.57	0.86	3
		ML_{low} (L μg DOC^{-1})	DOM	0.14	0.59	1.18	2.67
		ML_{high} (L μg C^{-1})	HA	0.36	0.36	0.87	1.2
			FA	0.2	0.14	0.57	0.59
		ML_{high} (L μg DOC^{-1})	DOM	0.11	0.17	0.32	1.36

should be isolated from the feedstock material (UW_0). This idea arises from the results previously described from the compost samples characterization that clearly showed an increase in both, the stabilization of organic matter and the chemical functions that are typical of HS throughout composting. However, a significant amount of FA and HA was found in UW_0 as compared to the matured compost, CUW. The yield increases from 2.2 g kg^{-1} (UW_0) to 3.3 g kg^{-1} (CUW) for FA and exhibits an unexpected decrease from 33.1 g kg^{-1} (UW_0) to 21.1 g kg^{-1} (CUW) for HA (Table 2). This atypical variation of HA and FA yields seems to indicate that the extraction/purification process (that was originally developed and optimized for soils) does not provide sufficient selectivity for isolating the HA and FA from fresh or not completely degraded biowastes.

The carbon content of HA and FA shows a decrease throughout composting, with values between 52.2% and 40.8% for FA and 59.8% and 54.5% for HA (Table 2). The atomic ratios of *C/N*, *O/C* and *H/C* from the FA and HA extracted from the compost samples at different stages of composting are presented in Table 2. The observed variations are similar to those reported in previous studies (Amir et al., 2010). The increase of *O/C* ratio, that is more pronounced for FA extracts, can be related to the increase of the oxygen containing moieties such as carboxylic and phenolic compounds (Hanc et al., 2019). The *H/C* ratio remains almost constant and does not seem to provide any information regarding the reactions that are taking place. The *C/N* ratio does not show a systematic decrease for the extracted FA and HA as for the corresponding compost samples (Table 2), particularly for the FA extracts where there is a tendency for an increase between UW_0 and CUW_{30}. This result can relate to the lack of selectivity of the extractions, considering that other organic substances may have been extracted besides HS, especially in the samples where HA or FA exists in small amounts.

3.2.3. Differential scanning calorimetry and thermogravimetric analysis of HS

DSC thermal characterization of FA and HA extracts from compost samples at different composting stages are presented in the supplementary material. The qualitative behaviour of the HS is similar to that of the compost. The DSC curves from the different materials exhibit marked differences in shape and height, leading to major variations in the values obtained by integration of the curves in the three temperature ranges (Table 2). This result may be due to the complexity of the extracted material and the large number of reactions that take place at close temperatures, making it rather difficult to isolate and quantify the contribution of each process. For FA samples the enthalpy associated with the decomposition of the recalcitrant substances (H_2) was higher than in case of HA (Table 2). This indicates that FA has a higher number of polar and oxygen-containing functional groups compared to HA. The enthalpy associated with the decomposition of the extra-recalcitrant substances (H_3) was higher for HA samples than for FA samples, apart from CUW. This fact may seem to be unexpected, due to the higher amount of nitrogen and aromatic structures in HA samples (Boguta et al., 2017).

The TGA and the corresponding DTG curves of both FA and HA (Figs. 1B and 1C) display two major processes and a secondary one at the lower temperatures. For the first temperature range (30–177 °C) the increase of WL_1 with the composting time is not meaningful considering the uncertainty associated with these results. The values of WL_2 (177–400 °C) tend to decrease with the composting time, indicating a progressive decomposition of simple and labile organic structures such as functional groups (carboxylic, methylene, alcohol, aldehydes, amides, amines and phenol groups), C-O of polysaccharides and simple aromatic bonds (biodegradable components) (Boguta et al., 2017). Simultaneously, the values of WL_3 (400–620 °C) tend to increase with the composting time, due to the increase of the amount of nitrogen-containing structures, long chain of hydrocarbons, refractory structures, aromatic, polyaromatic and polyheterocyclic structures, as well as C-C bond cleavage (Boguta et al., 2017). Regarding the results from FA, under air or N_2 atmospheres (Table 2), it is difficult to define a trend for the variation throughout composting (for each temperature range). In opposition, the results of the weight loss, WL_2, of HA under air or N_2 atmospheres (Table 2), show a decrease throughout composting, that is followed by the increase of WL_3. The increase of the residue is also a significant result indicating that it may be a consistent indicator of the increase of chemical stability of the HA and FA produced by composting.

3.2.4. Uv-vis, NMR and ATR-FTIR spectroscopy

The molar absorptivity coefficient at 280 nm, ε_{280} obtained for FA, HA and DOM was calculated from absorptivity data. The increase of this parameter throughout the composting process (Table 2) is related to the increase of the aromaticity of the extracts obtained throughout composting (Chin et al., 1994).

^{1}H NMR spectroscopy is a tool that can be used successfully to characterize the content and relative abundance of various chemical groups of HA and FA. Based on qualitative analysis, the ^{1}H NMR spectra of HA and FA were subdivided into five chemical shift regions, δ 0 – 3.0, δ 3.0 – 4.5, δ 4.7– 5.0, δ 5.0 – 6.0 and δ 6.0 – 9.0 ppm where the signals for protons associated to specific functional groups are registered. The relative areas of those signals, directly correlated to the number of protons that are present in that particular environment of the chemical entity are summarized in supplementary material. The ^{1}H NMR spectra were obtained from D_2O/NaOD solutions and the intense water peak that is always observed, reflects not only the water molecules retained by each sample but also those generated by D_2O exchange with the labile protons from carboxylic acids, phenols, and amines present in the molecular assemblies. For FA, the mole ratio of aliphatic versus aromatic protons (Table 2) increases slightly at the beginning of the composting process, and this can be due to a slight increase in the size of the alkyl chains, associated with a small decrease in the aromatic protons. This decrease may result from oxidation processes in the aromatic chains, more evident during maturation. The comparative analysis of the number of moles of protons in aliphatic carbon chains and in carbons adjacent to the oxygen atom shows a minor reduction in the beginning of the composting process (after 15 days). It remains practically unchanged, recovering the initial values at the end of the maturation process. For HA, the molar ratio of aliphatic versus aromatic protons (Table 2) steadily decreases during the composting process, which can result from the fragmentation of long carbon chains to generate progressively shorter units, with the subsequent loss of soluble small fragments. This trend seems to proceed during maturation to generate the final compost. This reduction in the length of the alkyl chains in HA is also supported by the reduction in the ratio of the number of hydrogen

atoms in these alkyl chains, when compared to the number of hydrogen atoms in carbons adjacent to oxygen, responsible for signals between 3 and 4.5 ppm in the ^{1}H NMR spectrum. The molecular ratio of water molecules (Table 2), when compared with the total number of aliphatic and aromatic protons, shows a marked increase for HA after 15 days of maturation, with minor alterations after this initial process. In contrast, FA shows a decrease in the ratio of water molecules versus aliphatic and aromatic protons after 15 days of maturation, followed by a significant increase during the final maturation period and the composting process. This demonstrates the high capacity of FA to retain water molecules in the compost material.

The ATR-FTIR spectra of the HA and FA extracts are shown in Figs. 2B and 2C. The information contained in these spectra is relevant regarding the monitoring of composting. The spectra display absorption bands typical of the FA and HA extracts. Those adsorption bands were identified considering previous studies (Baddi et al., 2004; González Pérez et al., 2004; Spaccini and Piccolo, 2009). Same intensity ratios as indicated for compost, $I_{1630/2925}$, $I_{1630/2845}$ and $I_{1530/2925}$ were used for HS (Table 2). The values of the three ratios obtained for the HA extracts increase throughout composting, suggesting that the extracted substances exhibit an increase of aromatic moieties and/or a decrease of aliphatic moieties. The values of these ratios for the FA extracts did not follow a regular trend. The values from the samples at the initial stages of composting even display a decrease. A significant increase of the ratios $I_{1630/2845}$ and $I_{1630/2925}$ was only observed for the last stage of composting, associated with the maturation stage. In opposition, the ratio $I_{1530/2925}$ did not change significantly along the entire process. This rather irregular variation throughout composting has already been reported by Amir et al. (Amir et al., 2010) and shows that these indexes may exhibit some limitations for the monitoring of the composting process.

3.2.5. Acid-base titrations

The acid-base properties of HA, FA and DOM extracts were performed by potentiometric titrations and discussed in detail by López et al. (López et al., 2021). This method enables to estimate relevant physico-chemical parameters, such as the protonation constant, K_i, and the abundance, M_i, of functional groups. The values of these parameters for the FA and HA extracts and DOM throughout composting (Table 2) were calculated by fitting the Eqs. (1 and 2) to the experimental data

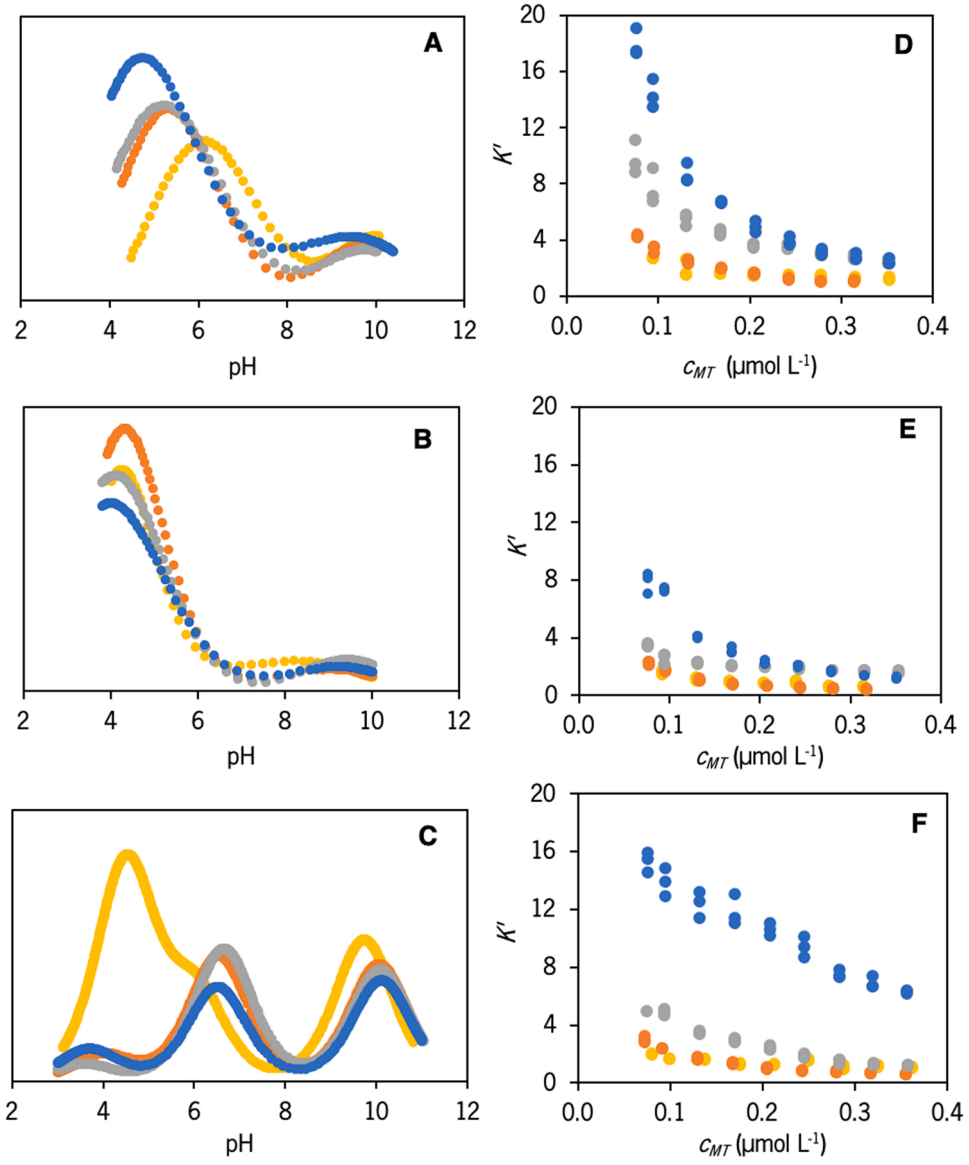

Fig. 3. Proton affinity distributions and experimental data for cadmium binding obtained for the HA (A, D), FA (B, E) and DOM (C, F) from the compost samples: (●) UW_0, (●) CUW_{15}, (●) CUW_{30}, (●) CUW.

(López et al., 2021).

$$Q = Q_0 + \frac{M_1}{1 + (K_1[H^+])^{m_1}} + \frac{M_2}{1 + (K_2[H^+])^{m_2}} \quad (1)$$

$$Q = Q_0 + \frac{M_1}{1 + (K_1[H^+])} + \frac{M_2}{1 + (K_2[H^+])} + \frac{M_3}{1 + (K_3[H^+])} \quad (2)$$

where K_i is the protonation constant of the different groups, M_i is the abundance of each type of acid site, and Q_0 is the charge due to occupation of the acid sites by cations that must be displaced by protonation.

Two types of acid sites, carboxylic-type, K_1 and phenolic-type, K_2 were identified for HA and FA extracts (Figs. 3A and 3B). The abundance of the carboxylic groups, M_1, showed a significant increase for both extracts, whereas the abundance of phenolic groups, M_2, increased for HA and decreased for FA. The decrease of M_2 for FA can be a consequence of a more effective oxidation of the phenolic groups to the corresponding carboxylic acids comparatively to the rate of formation of new phenolic groups. The decrease of the pK_1 values (from 6.09 to 4.43 for HA and from 4.24 to 3.99 for FA) may be directly related to the rise of the number of aromatic structures. With respect to pK_2 this effect is also found for the HA extracts, decreasing from 10.17 to 9.81. For the FA extracts an increase was observed for pK_2 values from 8.38 to 9.38.

The three types of sites were identified for DOM corresponding to: i) carboxylic groups in amino acids, ii) carboxylic groups in organic acids and iii) phenolic hydroxyl groups, hydroxyl in carbohydrate units and amino groups from amino acids (Fig. 3C). The variation trend of the acidity constants and abundance of the acidic groups is not constant throughout composting. The large value of M_1 obtained in UW_0 can be attributed to the presence of amino acids that are largely consumed in the first stage of composting. The value of M_2 tends to increase, despite the small decrease observed for CUW. For M_3 a continuous decrease is observed, similar to that observed for M_2 of FA, which confirms the presence of FA, in the equilibrium solutions. This statement is supported by the similarity of the values of pK_2 of FA and pK_3 of DOM.

3.2.6. Metal binding extent

The evaluation of the binding of metal ions by the HS extracts may be used for the characterization of these substances, as the extent of this process is strongly associated with the nature of the functional groups present and with the structure of molecular aggregates formed by HS. Besides the chemical characterization purposes, the complexing ability of the DOM is also relevant to understand the fate of environmental pollutants (Buffle and DeVitre, 1994). The organic substances present in DOM are the most mobile and therefore the most accessible to participate in several equilibria in environment.

Results obtained for the binding of cadmium by HA, FA and DOM are shown in Figs. 3D to 3F. The plots represent the average complexation constant K' as a function of the total cadmium concentration, c_{MT}, (in mol L^{-1}), where K' values were calculated as the ratio c_{ML}/c_M, where c_{ML} is the metal complex concentration and c_M the free metal concentration. This ratio is related to the stability constant of metal complexes. From plots in Figs. 3D to 3F it is observed that all curves follow the same order, from UW_0 (at the bottom) to CUW (at the top). The shape of these curves (decreasing K' with increasing c_{MT}) is typical of heterogeneous materials, where the binding by the strongest groups occurs for the first additions of Cd^{2+}. The decrease of the average value of K' occurs progressively with the increasing involvement of the weaker binding groups due to the occupation of the stronger sites. To facilitate the comparison between the extracts at different composting stages the values of ML_{low} and ML_{high} were calculated (Table 2). These quantities correspond to K'/c_L, where c_L represents the concentration of organic matter for a low (0.10 μmol L^{-1}) and a high (0.30 μmol L^{-1}) concentration of total metal in solution. The values of ML_{low} and ML_{high} are a measure of the average binding ability of the strongest groups and of the overall groups, respectively. Both parameters displayed a gradual increase throughout composting in all extract (with only one exception, ML_{high} of the FA extract of CUW_{15}, which is lower than UW_0). However, the differences between the values ML_{high} are more relevant, indicating that the molecular changes associated with composting impose pronounced modifications on the strong complexing groups. These results confirm what was previously discussed, that during the maturation period there is an increase of the number of strong binding sites of the extracts, while the number of weak binding sites does not seem to vary.

3.3. Multi – block data analysis

The main premise of this work is to determine which are the most suitable techniques and parameters to characterize the evolution of compost throughout the composting process. This is a complex task due to the diversity of methodologies used for this purpose that requires the use of an adequate statistical tool like the multi-blocks analysis. The ComDim evaluation was applied to explore the multiple data blocks defined using results from the chronological characterization of a compost (CUW) and of its extracts (HA, FA and DOM). The analysis was performed separating the results from each sample (compost, HA, FA and DOM) in two groups: the first (blocks 1, 3, 5, and 7) with data related to the elemental composition of each sample (comprising data from elemental analysis and content of ionic species) and the second (blocks 2, 4, 6, and 8) with data related to the molecular structure of species in each sample (comprising data from yield of HA and FA extractions, pH, CEC, EC, UV–vis, ATR-FTIR, ^{1}H NMR, TGA, DSC, acid-base and metal binding titrations). Results of the solid compost at different composting stages are in blocks 1 and 2, of DOM are in blocks 3 and 4, of HA are in blocks 5 and 6, and of FA are in blocks 7 and 8. Data included in each block is presented in Tables 1 and 2. Results obtained from ComDim analysis, with the informative graphics of the saliences, scores, and loadings are shown in Figs. 4A to 4C, respectively. Eight common components, CCs, were computed on this ComDim evaluation and considered sufficient to take into account all sources of variation in the eight data blocks (Fig. 4A). No significant information was observed in saliences from CCs 4–8, and compared to the CC1, an inferior variability was observed in the CCs 2 and 3. On CC1 it is possible to suggest that an inter-block relationship was achieved, although blocks 4, 6 (corresponding to the results related to molecular structure of DOM and HA) and block 5 (corresponding to the elemental composition of HA), presented higher saliences. This outcome indicates that results from analytical parameters related either to the elemental composition or to molecular structure of the solid compost, DOM, HA or FA are able to distinguish samples obtained at the different stages of composting. The ComDim scores on CC1 (Fig. 4B) show the chronological development of the solid compost and of its extracts. The samples (compost and extracts) from the feedstock (UW_0), with more negative scores, were differentiated from those of the matured compost (CUW), with more positive scores. The samples from CUW_{15} and CUW_{30} present intermediate scores. The relative importance of the different analytical techniques for monitoring composting can be recognized from the loadings plot in Fig. 4C. The variables that display higher loadings correspond to the analytical parameters that are more successful to distinguish CUW and the lower loadings correspond to the analytical parameters that are more successful to distinguish UW_0 from the remaining samples.

For the identification of the techniques and parameters that were more successful, the variables were divided in 3 ranges according to the absolute values of the loadings, $|L| > 0.8$, $0.4 < |L| < 0.8$ and $|L| < 0.4$. Besides, the variation trend of the analytical parameters was examined. The selected analytical parameters, that display at least for one sample $|L| > 0.4$ and vary in a single way along the process, are listed in supplementary material. With respect to the elemental characterization of the solid compost and its extracts the most relevant parameters were: C, C_{oxi} and C/N for compost; C_{oxi}, DOC, PO_4^{3-} and NO_2^- for DOM and C, N, H, C/N and O/C for HS extracts (HA and FA). Concerning the parameters related to molecular structure, ε_{280} was relevant for DOM and HS

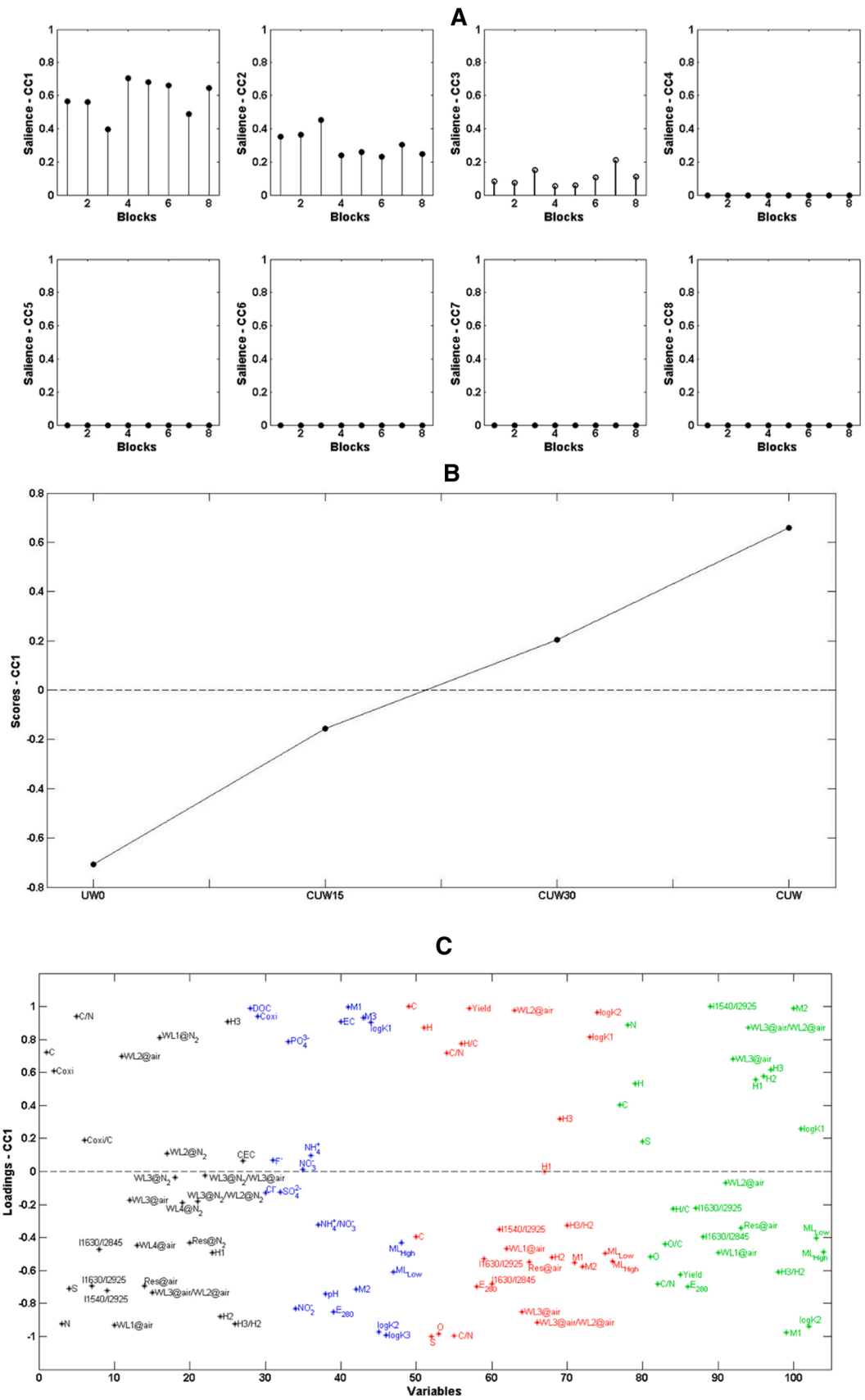

Fig. 4. ComDim results. Saliences from CC1 to CC8: blocks 1, 3, 5, and 7 obtained from data of elemental composition and blocks 2, 4, 6, and 8 obtained from data related to molecular structure, where block 1, 2 are from solid compost; 3, 4 are from DOM; 5, 6 are from HA and 7, 8 are from FA (A); Scores of CC1 (B); Loadings of the CC1, are displayed in different colours according to the sample nature: solid compost (•), DOM (●), HA (●) and FA (●) (C).

extracts. The *pH* and *EC* were also relevant for DOM characterization. The ratios $I_{1630/2845}$, $I_{1630/2925}$ and $I_{1540/2925}$ (from the ATR-FTIR analysis) were meaningful for compost, whereas for HS extracts only $I_{1630/2845}$ was adequate. The variables H_2 and H_3 /H_2 (from DSC) were relevant for compost whereas for the HS extracts H_1 and H_3 /H_2 were significant. The variables WL_1@*air*, WL_2@*air*, WL_4@*air*, *Res* @*air*, WL_3@*air*/WL_2@*air*, WL_1@N_2 and *Res* @N_2 (from TGA analysis) were relevant for compost, while for HS extracts just WL_1@*air* and WL_3@*air* were meaningful. The acid-base parameters M_1, M_2, M_3 and $log\ K_1$ of DOM and M_1, M_2 and log K_2 of HS extracts were relevant. Regarding the metal binding parameters both ML_{low} and ML_{high} were relevant for DOM, whereas for the HS extracts only the ML_{high} were meaningful.

4. Conclusions

As the different analytical methods track distinctive features of materials, parameters related either with the elemental composition or with structural features of compost exhibit different variation patterns throughout composting. An inter-block relationship between results from all samples, organized in eight blocks according to the nature of the samples and of the analytical information, was established by a ComDim analysis. Besides the identification of the parameters and techniques that contributed more significantly for the samples discrimination, this analysis demonstrates that compost evolution can be monitored alternatively by means of solid samples, humic extracts or dissolved organic matter. These results can be generalized to composts of different origins by performing further experiments with varied raw materials.

E-supplementary data of this work can be found in the online version of the paper.

Declaration of Competing Interest

The authors declare that they have no known competing financial interests or personal relationships that could have appeared to influence the work reported in this paper.

Acknowledgments

This work was financially supported by the Interreg VA Spain-Portugal Programme (EU) through the project Res2ValHum (0366_RES2VALHUM_1_P). A.C. Silva acknowledges receipt of a PhD grant (UMINHO/BD/40/2016) financed by the Operational Program Norte 2020, Portugal (through the Project "NORTE-08–5369-FSE-000033"). Thanks are due to Fundação para a Ciência e Tecnologia (FCT, Portugal) and FEDER (European Fund for Regional Development)-COMPETE-QRENEU for financial support through the Chemistry Research Centre of the University of Minho, Portugal (UID/QUI/00686/2020). J.Antelo, R.López and S.Fiol are also grateful for the financial support provided by Xunta de Galicia - Consellería de Educación e Ordenación Universitaria de Galicia, Spain (Consolidation of Competitive Groups of Investigation; GI-1245, ED431C 2018/12 and CRETUS AGRUP2015/02, ref. 2018-PG10). P. Valderrama, thanks CNPq, Brazil (process 306606/2020–8). We would also like to acknowledge to Lipor (Serviço Intermunicipalizado de Gestão de Resíduos do Grande Porto, Portugal) for providing the samples of compost used in this work.

Appendix A. Supporting information

Supplementary data associated with this article can be found in the online version at doi:10.1016/j.psep.2022.06.057.

References

Amir, S., Jouraiphy, A., Meddich, A., El Gharous, M., Winterton, P., Hafidi, M., 2010. Structural study of humic acids during composting of activated sludge-green waste: elemental analysis, FTIR and ^{13}C NMR. J. Hazard. Mater. 177, 524–529. https://doi.org/10.1016/j.jhazmat.2009.12.064.

Awasthi, S.K., Sarsaiya, S., Awasthi, M.K., Liu, T., Zhao, J., Kumar, S., Zhang, Z., 2020. Changes in global trends in food waste composting: Research challenges and opportunities. Bioresour. Technol. 299, 122555 https://doi.org/10.1016/j.biortech.2019.122555.

Azim, K., Soudi, B., Boukhari, S., Perissol, C., Roussos, S., Thami Alami, I., 2018. Composting parameters and compost quality: a literature review. Org. Agric. 8, 141–158. https://doi.org/10.1007/s13165-017-0180-z.

Baddi, G.A., Hafidi, M., Cegarra, J., Alburquerque, J.A., Gonzálvez, J., Gilard, V., Revel, J.C., 2004. Characterization of fulvic acids by elemental and spectroscopic (FTIR and 13C NMR) analyses during composting of olive mill wastes plus straw. Bioresour. Technol. 93, 285–290. https://doi.org/10.1016/j.biortech.2003.10.026.

Bernal, M.P., Alburquerque, J.A., Moral, R., 2009. Composting of animal manures and chemical criteria for compost maturity assessment. A review. Bioresour. Technol. 100, 5444–5453. https://doi.org/10.1016/j.biortech.2008.11.027.

Boguta, P., Sokołowska, Z., Skic, K., 2017. Use of thermal analysis coupled with differential scanning calorimetry, quadrupole mass spectrometry and infrared spectroscopy (TG-DSC-QMS-FTIR) to monitor chemical properties and thermal stability of fulvic and humic acids. PLoS ONE 12, 1–18. https://doi.org/10.1371/journal.pone.0189653.

Bouveresse, D.J.-R., Pinto, R.C., Schmidtke, L.M., Locquet, N., Rutledge, D.N., 2011. Identification of significant factors by an extension of ANOVA–PCA based on multiblock analysis. Chemom. Intell. Lab. Syst. 106, 173–182. https://doi.org/10.1016/j.chemolab.2010.05.005.

Buffle, J., DeVitre, R.R., 1994. Chemical and biological regulation of aquatic systems. Lewis Publ., Boca Raton.

Cariou, V., Bouveresse, D.J.-R., Qannari, E.M., Rutledge, D.N., 2019. ComDim methods for the analysis of multiblock data in a data fusion perspective. In: Data Handling in Science and Technology. Elsevier, pp. 179–204. https://doi.org/10.1016/B978-0-444-63984-4.00007-7.

Cegarra, J., Garcia, D., Navarro, A., Bernal, M.P., 1994. Effects of heat on the alkali extraction of humic substances from peat. Commun. Soil Sci. Plant Anal. 25 https://doi.org/10.1080/00103629409369218.

Cerda, A., Artola, A., Font, X., Barrena, R., Gea, T., Sánchez, A., 2018. Composting of food wastes: Status and challenges. Bioresour. Technol. 248, 57–67. https://doi.org/10.1016/j.biortech.2017.06.133.

Chin, Y.-P., Aiken, G., O'Loughlin, E., 1994. Molecular weight, polydispersity, and spectroscopic properties of aquatic humic substances. Environ. Sci. Technol. 28, 1853–1858. https://doi.org/10.1021/es00060a015.

Dell'Abate, M.T., Benedetti, A., Sequi, P., 2000. Thermal methods of organic matter maturation monitoring during a composting process. J. Therm. Anal. Calorim. 61, 389–396. https://doi.org/10.1023/A:1010157115211.

L.F. Diaz, C.G. Golueke, G.M. Savage, L.L. Eggerth, Composting and recycling municipal solid waste, 2020.

Droussi, Z., D'orazio, V., Provenzano, M.R., Hafidi, M., Ouatmane, A., 2009. Study of the biodegradation and transformation of olive-mill residues during composting using FTIR spectroscopy and differential scanning calorimetry. J. Hazard. Mater. 164, 1281–1285. https://doi.org/10.1016/j.jhazmat.2008.09.081.

El Ghaziri, A., Cariou, V., Rutledge, D.N., Qannari, E.M., 2016. Analysis of multiblock datasets using ComDim: Overview and extension to the analysis of (K + 1) datasets: ComDim analysis: overview and extension. J. Chemom. 30, 420–429. https://doi.org/10.1002/cem.2810.

Fernández, J.M., Plaza, C., Polo, A., Plante, A.F., 2012. Use of thermal analysis techniques (TG-DSC) for the characterization of diverse organic municipal waste streams to predict biological stability prior to land application. Waste Manag. 32, 158–164. https://doi.org/10.1016/j.wasman.2011.08.011.

Fuentes, M., González-Gaitano, G., García-Mina, J.M., 2006. The usefulness of UV–visible and fluorescence spectroscopies to study the chemical nature of humic substances from soils and composts. Org. Geochem. 37, 1949–1959. https://doi.org/10.1016/j.orggeochem.2006.07.024.

Fuentes, M., Baigorri, R., González-Gaitano, G., García-Mina, J.M., 2007. The complementary use of 1H NMR, ^{13}C NMR, FTIR and size exclusion chromatography to investigate the principal structural changes associated with composting of organic materials with diverse origin. Org. Geochem. 38, 2012–2023. https://doi.org/10.1016/j.orggeochem.2007.08.007.

Galceran, J., Companys, E., Puy, J., Cecilia, J., Garces, J.L., 2004. AGNES: a new electroanalytical technique for measuring free metal ion concentration. J. Electroanal. Chem. 566, 95–109. https://doi.org/10.1016/j.jelechem.2003.11.017.

Gigliotti, G., Kaiser, K., Guggenberger, G., Haumaier, L., 2002. Differences in the chemical composition of dissolved organic matter from waste material of different sources. Biol. Fertil. Soils 36, 321–329. https://doi.org/10.1007/s00374-002-0551-8.

Gigliotti, G., Macchioni, A., Zuccaccia, C., Giusquiani, P.L., Businelli, D., 2003. A spectroscopic study of soil fulvic acid composition after six-year applications of urban waste compost. Agronomie 23, 719–724. https://doi.org/10.1051/agro:2003048.

González Pérez, M., Martin-Neto, L., Saab, S.C., Novotny, E.H., Milori, D.M.B.P., Bagnato, V.S., Colnago, L.A., Melo, W.J., Knicker, H., 2004. Characterization of humic acids from a Brazilian Oxisol under different tillage systems by EPR, 13C NMR, FTIR and fluorescence spectroscopy. Geoderma 118, 181–190. https://doi.org/10.1016/S0016-7061(03)00192-7.

Guo, X., Liu, H., Wu, S., 2019. Humic substances developed during organic waste composting: formation mechanisms, structural properties, and agronomic functions. Sci. Total Environ. 662, 501–510. https://doi.org/10.1016/j.scitotenv.2019.01.137.

Hanc, A., Enev, V., Hrebeckova, T., Klucakova, M., Pekar, M., 2019. Characterization of humic acids in a continuous-feeding vermicomposting system with horse manure. Waste Manag. 99, 1–11. https://doi.org/10.1016/j.wasman.2019.08.032.

Harada, Y., Inoko, A., 1980. Relationship between cation-exchange capacity and degree of maturity of city refuse composts. Soil Sci. Plant Nutr. 26, 353–362. https://doi.org/10.1080/00380768.1980.10431220.

Haug, R.T., 1993. The Practical Handbook of Compost Engineering, 1st ed. Routledge. https://doi.org/10.1201/9780203736234.

Hsu, J.H., Lo, S.L., 1999. Chemical and spectroscopic analysis of organic matter transformations during composting of pig manure. Environ. Pollut. 104, 189–196. https://doi.org/10.1016/S0269-7491(98)00193-6.

Huang, G.F., Wong, J.W.C., Wu, Q.T., Nagar, B.B., 2004. Effect of C/N on composting of pig manure with sawdust. Waste Manag. 24, 805–813. https://doi.org/10.1016/j.wasman.2004.03.011.

Inbar, Y., Chen, Y., Hadar, Y., 1989. Solid-state carbon-13 nuclear magnetic resonance and infrared spectroscopy of composted organic matter. Soil Sci. Soc. Am. J. 53, 1695–1701. https://doi.org/10.2136/sssaj1989.03615995005300060014x.

Inbar, Y., Hadar, Y., Chen, Y., 1992. Characterization of humic substances formed during the composting of solid wastes from wineries. Sci. Total Environ. 113, 35–48. https://doi.org/10.1016/0048-9697(92)90015-K.

Kaiser, M., Ellerbrock, R.H., 2005. Functional characterization of soil organic matter fractions different in solubility originating from a long-term field experiment. Geoderma 127, 196–206. https://doi.org/10.1016/j.geoderma.2004.12.002.

Kaza, S., Yao, L., Bhada-Tata, P., Woerden, F.V., 2018. What a Waste 2.0: A Global Snapshot of Solid Waste Management to 2050. World Bank Group.

Li, R., Xu, K., Ali, A., Deng, H., Cai, H., Wang, Q., Pan, J., Chang, C.-C., Liu, H., Zhang, Z., 2020. Sulfur-aided composting facilitates ammonia release mitigation, endocrine disrupting chemicals degradation and biosolids stabilization. Bioresour. Technol. 312, 123653 https://doi.org/10.1016/j.biortech.2020.123653.

López, R., Fiol, S., Antelo, J.M., Arce, F., 2003. Analysis of the effect of concentration on the acid-base properties of soil fulvic acid. Conform. Chang., Colloids Surf. A: Physicochem. Eng. Asp. 226, 1–8. https://doi.org/10.1016/S0927-7757(03)00358-3.

López, R., Antelo, J., Silva, A.C., Bento, F., Fiol, S., 2021. Factors that affect physicochemical and acid-base properties of compost and its potential use as a soil amendment. J. Environ. Manag. 300, 113702 https://doi.org/10.1016/j.jenvman.2021.113702.

Melis, P., Castaldi, P., 2004. Thermal analysis for the evaluation of the organic matter evolution during municipal solid waste aerobic composting process. Thermochim. Acta 413, 209–214. https://doi.org/10.1016/j.tca.2003.09.026.

Murphy, J., Riley, J.P., 1962. A modified single solution method for the determination of phosphate in natural waters. Anal. Chim. Acta 27, 31–36. https://doi.org/10.1016/S0003-2670(00)88444-5.

Ouatmane, A., Provenzano, M.R., Hafidi, M., Senesi, N., 2000. Compost maturity assessment using calorimetry, spectroscopy and chemical analysis. Compost Sci. Util. 8, 124–134. https://doi.org/10.1080/1065657X.2000.10701758.

Piccolo, A., Mirabella, A., 1987. Molecular weight distribution of peat humic substances extracted with different inorganic and organic solutions. Sci. Total Environ. 62, 39–46. https://doi.org/10.1016/0048-9697(87)90479-7.

Piccolo, A., Zaccheo, P., Genevini, P.G., 1992. Chemical characterization of humic substances extracted from organic-waste-amended soils. Bioresour. Technol. 40, 275–282. https://doi.org/10.1016/0960-8524(92)90154-P.

Plaza, C., Senesi, N., Polo, A., Brunetti, G., 2005. Acid-base properties of humic and fulvic acids formed during composting. Environ. Sci. Technol. 39, 7141–7146. https://doi.org/10.1021/es050613h.

Qannari, E.M., Wakeling, I., Courcoux, P., MacFie, H.J.H., 2000. Defining the underlying sensory dimensions. Food Qual. Prefer. 11, 151–154. https://doi.org/10.1016/S0950-3293(99)00069-5.

Rocha, L.S., Companys, E., Galceran, J., Carapuça, H.M., Pinheiro, J.P., 2010. Evaluation of thin mercury film rotating disk electrode to perform absence of gradients and Nernstian equilibrium stripping (AGNES) measurements. Talanta 80, 1881–1887. https://doi.org/10.1016/j.talanta.2009.10.038.

Rocha Baqueta, M., Coqueiro, A., Henrique Março, P., Mandrone, M., Poli, F., Valderrama, P., 2021. Integrated ^{1}H NMR fingerprint with NIR spectroscopy, sensory properties, and quality parameters in a multi-block data analysis using ComDim to evaluate coffee blends. Food Chem., 129618 https://doi.org/10.1016/j.foodchem.2021.129618.

Rosa, L.N., de Figueiredo, L.C., Bonafé, E.G., Coqueiro, A., Visentainer, J.V., Março, P.H., Rutledge, D.N., Valderrama, P., 2017. Multi-block data analysis using ComDim for the evaluation of complex samples: characterization of edible oils. Anal. Chim. Acta 961, 42–48. https://doi.org/10.1016/j.aca.2017.01.019.

Saharinen, M.H., 1998. Evaluation of changes in CEC during composting. Compost Sci. Util. 6, 29–37. https://doi.org/10.1080/1065657X.1998.10701938.

Søberg, L.C., Winston, R., Viklander, M., Blecken, G.-T., 2019. Dissolved metal adsorption capacities and fractionation in filter materials for use in stormwater bioretention facilities. Water Res. X 4, 100032. https://doi.org/10.1016/j.wroa.2019.100032.

Som, M.P., Lemée, L., Amblès, A., 2009. Stability and maturity of a green waste and biowaste compost assessed on the basis of a molecular study using spectroscopy, thermal analysis, thermodesorption and thermochemolysis. Bioresour. Technol. 100, 4404–4416. https://doi.org/10.1016/j.biortech.2009.04.019.

Spaccini, R., Piccolo, A., 2009. Molecular characteristics of humic acids extracted from compost at increasing maturity stages. Soil Biol. Biochem. 41, 1164–1172. https://doi.org/10.1016/j.soilbio.2009.02.026.

Sumner, M.E., Miller, W.P., 1996. Cation exchange capacity and exchange coefficients. In: Sparks, D.L., Page, A.L., Helmke, P.A., Loeppert, R.H., Soltanpour, P.N., Tabatabai, M.A., Johnston, C.T., Sumner, M.E. (Eds.), Methods of Soil Analysis Part 3—Chemical Methods. Soil Science Society of America, American Society of Agronomy, Madison, WI, USA, pp. 1201–1229. https://doi.org/10.2136/sssabookser5.3.c40.

Swift, R.S., 1996. Organic Matter Characterization. In: Sparks, D.L., Page, A.L., Helmke, P.A., Loeppert, R.H., Swift, R.S. (Eds.), Methods of Soil Analysis Part 3—Chemical Methods. Soil Science Society of America, American Society of Agronomy, pp. 1011–1069. https://doi.org/10.2136/sssabookser5.3.c35.

The European Parliament and the Council of the European Union, Directive 2008/98/EC of the European Parliament and of the Council of 19 November 2008 on waste, 2008. http://ec.europa.eu/environment/waste/framework/.

The European Parliament and the Council of the European Union, Directive (EU) 2018/851 of the European Parliament and of the Council of 30 May 2018 amending Directive 2008/98/EC on waste, 2018. https://eur-lex.europa.eu/legal-content/EN/TXT/?qid=1530557218036&uri=CELEX:32018L0851.

Walkley, A., 1947. A critical examination of a rapid method for determining organic carbon in soils – effect of variations in digestion conditions and of inorganic soil constituents. Soil Sci. 63, 251–264. https://doi.org/10.1097/00010694-194704000-00001.

Wang, K., Li, X., He, C., Chen, C.L., Bai, J., Ren, N., Wang, J.Y., 2014. Transformation of dissolved organic matters in swine, cow and chicken manures during composting. Bioresour. Technol. 168, 222–228. https://doi.org/10.1016/j.biortech.2014.03.129.

Wu, J., Zhao, Y., Zhao, W., Yang, T., Zhang, X., Xie, X., Cui, H., Wei, Z., 2017. Effect of precursors combined with bacteria communities on the formation of humic substances during different materials composting. Bioresour. Technol. 226, 191–199. https://doi.org/10.1016/j.biortech.2016.12.031.

Xu, Z., Li, R., Wu, S., He, Q., Ling, Z., Liu, T., Wang, Q., Zhang, Z., Quan, F., 2022. Cattle manure compost humification process by inoculation ammonia-oxidizing bacteria. Bioresour. Technol. 344, 126314 https://doi.org/10.1016/j.biortech.2021.126314.